MAGNETIC SPRING IN OSCILLATING MIRROR LINEAR SCANNER

FOR SATELLITE CAMERA

by G. THOMIN

of the Centre National d'Etudes Spatiales (CNES)

and C. FOUCHE

of the Société Européenne de Propulsion (SEP)

SUMMARY

One of the main difficulties encountered in the development of a multispectral scanner is the realisation of an oscillating mechanical device. This paper presents a magnetic device which is characterized by the absence of friction. The main developments concern the analysis of magnetic forces. A preliminary project of a device which could be used in a satellite is presented.

INTRODUCTION

The multispectral pictures of the earth taken by satellite are of great interest for the understanding of natural phenomena. The device presented here has the potential qualities which enable us to envisage in the near future an increase in the performance of scanners.

A mirror placed in the lens's space of a telescope is animated by a linear oscillation, thus means that the diagram of angular movement has a triangular shape.

The characteristics used as a basis for elaboration of the project are the following :

- useful angular amplitude = $\pm$ 4.4. degrees
- oscillation frequency = 8 Hertz
- pupil/beam diameter = 280 mm

The following performances are required :

- Linearity better than $\pm$ 0.5 %
- Scanning efficiency on away movement 0.35
- reproductibility of the movement less than $4 \cdot 10^{-6}$ radian
- pivoting precession less than $4 \cdot 10^{-6}$ radian

This paper is based on work carried out in collaboration between the CNES and the SEP, the magnetic device presented is subject of patent pending.

PRINCIPLES OF THE MAGNETIC SPRING

The linear oscillation of the mirror is obtained by a magnetic thrusting effect on both ends of the useful angular movement. The magnetic thrusts are associated with a pivot without spring torque effect using an active electro-magnetic bearing. Consequently, the rotor is guided in its oscillation only by the magnetic forces. The drawing of the principle of a magnetic thrust is presented in figure 1. A highly induced saturation ferro-magnetic strip moves between two armatures so that the magnetic circuit gaps are small and constant. The gaps do not vary when the strip is moved along the whole length of the armature. But, at the end of the run, the magnetic resistance of the gaps increases abruptly. As a result there appears at both ends a reaction force, F_R, which is proportional to the derivative of the magnetic resistance.

$$F_R = \frac{1}{2} \varphi^2 \frac{\partial R}{\partial \theta}$$

φ = magnetic flux of the gaps
R = magnetic resistance of the gaps
θ = rotation angle of the mirror

Figure 2 represents the outlook diagram of Torque and diagram of the angular movement in relation to time.

The distribution of the magnetic field lines goes from a symetric distribution at the center to asymmetric distributions at both ends of the course (see figure 1). The result is a assymmetry in the pressure of forces generated by the magnetic field on both lateral faces of the strip and the appearance of a return-force towards the center. The pressure on the contours of the strip is calculated by the formula :

$$df = \frac{B^2}{2\mu o} dS$$

where B = magnetic induction
dS = elementary section
$\mu o = 4 \pi 10^{-7}$

However, as in all magnetic attraction systems, the stiffness of the re-centering described above has for result, a strong unstable stiffness in the direction of the magnetic flux circulation.

In the central position, the strip has an unstable balance which means that a shift in its position creates a force which tends to increase this shift. This instability is produced by an increase in magnetic field density lines at the end of the strip closest to the armature and inversely at the other end. The presence of an unstable stiffness is the major difficulty in the setting-up of the magnetic thrust, this difficulty being overcome by using SEP electromagnetic bearing which has a large position stiffness.

Moreover, a ferror-magnetic material used for the armature having a weaker saturation induction than that of the strip contributes to a notable instability reduction.

The magnetic thrust intrinsic instability has been the object of a theoretical survey using a numerical finite elements method to calculate magnetic field distribution.

As an example, the visualisation of the magnetic field lines near the gap is represented in figures 3 and 4. On figure 3, the materials (ferro-cobalts) are identical for the strip and the armature. On figure 4, the strip is of ferro - cobalt (B_S = 2,4 Tesla) and the armature is ferro-nickel (B_S = 1,3 Tesla). It would appear that the use of material with a low induction saturation has the effect of reducing the density of field lines on the end of the strip, and that of creating a saturated zone in the armature near the gap. Depending on the proximity of this strip, this saturable zone increases. In comparison with the figure 3, the case plotted on figure 4 having for effect the instability reduction with a ratio of 120%. This phenomenom has been confirmed by laboratory experiments.

PRELIMINARY SURVEY MODEL

To validate the principle of the magnetic thrust, an experimental oscillating assembly was constructed. The overall view of this is represented in picture 5. The experimental assembly was constructed around a precision pivot by conical air bearing and has two devices for magnetic thrusts situated at both ends of an oscillating arm. The magnetic circuit of the thrusts is represented in figure 9, the armature a_1, a_2 in cylindrical form, are connected to the rotor represented in picture 6, the strips b_1, b_2, b_3, b_4 are mounted on two mechanical gap alignment systems (photo 7), the whole of the pieces making up a magnetic thrust is represented by picture 8. The main parameters of the experimental mount are as follows :

rotor inertia	:	0,15 m2 kg
Useful angular amplitude	:	$\pm$ 5 degrees
Frequency	:	2.2. Hz
Maximum Torque Thrust capacity	:	2 N m

In a dynamic situation of the thrusts reaction, torque is represented in figure 10 (measured by accelerometer). Figure 11 represents the angular rotation in relation to time, the effect of linearisation is obtained with a scanning efficiency nearer 32% for a linearity better than 1%. To simplify this experiment, the armature have been produced in a solid magnetic material and the result is large eddy current losses per cycle in the order of 20% compensated for each cycle by a precise torque impulsion controlled in a servo-loop.

A scanning reproductibility measure was produced by a laser device and photodiodes, the whole measuring apparatus is shown in figures 12 and 13. The histogram of oscillation angular variations of the mirror is shown in figure 14. The reproduction error is at most 3.10^{-6} radian and 78% of these errors are less than 10^{-6} radian.

These results have enabled more important work to be started leading to a preliminary project for a complete scanner model.

REACTION FORCES OF THE MAGNETIC THRUSTS

Two tests assemblies for the magnetic thrusts have been produced to analyse, as precisely as possible, the reaction forces of the magnetic thrusts. Picture 15 shows the test apparatus for measuring reaction torque and picture 16 shows the testing apparatus for the unstable forces. These tests have facilitated the verification fo the influence of the main dimensional paramaters of magnetic circuit :

The increase in the breadth of the strip has for effect not only an increase of the torque capacity but also increase in the unstable force.

The reduction of the gap diminishes the foot curvatum reaction torque diagram and increases the instability.

The use of saturable materials on the armature reduces instability.

The method of flux generation clearly influences the reaction torque capacity ; in the event of powering, the armature with constant magnetic potential, the flux decreases quickly when the strip leaves the armature, which reduces the torque capacity. On the other hand, a constant flux generation realized by placing additionals gaps in series in the magnetic circuit allows to increase notably the capacity of torque without increasing the instability very much.

Parts of experimental results are plotted on the figures 17,18,19,20.

PRELIMINARY SCANNER PROJECT

Figure 21 shows a design of a preliminary project of a mirror oscillating from 280 mm x 320 mm, the magnetic thrusts are formed by two strips of ferro-cobalt 60 mn long, 40 mn wide and 3.5 mn thick, fixed at the end of the long axis of the mirror, the ferro-nickel armatures have been laminated to reduce eddy current losses. The provision of flux is provided for by magnets of samarium-cobalt and is closed to the stator by a piece of soft iron.

The magnetic bearings are placed at the ends of the small axis of the mirror, they are formed by :

- a set of electromagnets acting over the five degrees of freedom

- a detection set of the position of the rotor on the five degrees of freedom . They are inductive detectors supplied at 100 KHz with demodulator.

The degree of precision of this detection set is considerable : the value of rotation noise is less than a hundredth of a micron.

- an electronic set for five degrees servo-loop.

The active electomagnetic bearings offer the advantage of having a long experience at the SEP, both for space applications (Spacelab) as well as industrial applications. The choice of these instruments, to assure the rotation of the mirror, is justified by the following requirements.

- guiding precision of the rotation axis. This axis must be maintained in a conical semi-angle less than 4.10^{-6} radian.

- great stiffness of 5 degrees of freedom in pivoting.
This quality is of prime necessity : the precision of rotation is to be preserved under the influence of unstable forces of thrusts, these forces acting by axial translation and transverse rotation in the mirror.

- elimination of all frictions

- absence of spring rotating torque and low drag torque

An arch of light alloy allows to connect rigidly the bearing and the magnetic thrusts, especially following the strong instability directions of the thrusts.

The reduction in the mirrors inertia around its rotation axis is essential for reducing the torque capacity of the thrusts and their transversal instability.

Considering a linear torque-angle characteristic for the thrusts, formulas for the torque capacity and for the reaction stiffness torque can be established :

$$Cmax = Ir \times \frac{Teta}{2\pi} \cdot \frac{(2\pi\ F)^2}{Te(0{,}5-Te)}$$

$$Rm = Ir. \left(\frac{2\pi F}{0{,}5-Te}\right)^2$$

Ir = rotor inertia

Teta = useful angular scanning

F = Oscillation frequency

Te = Scanning efficiency on away movement

Rm = Magnetic stiffness of the thrusts assumed like constants

Cmax = Capacity of the torque thrusts

In the preliminary project configuration in figure 21, the oscillation characteristics have been extrapolated from the results of the experimental survey of the thrusts. These results are shown in figure 22 . The rotor inertia is 0.04 m2 Kg, and scanning efficiency is 0.36 with ± 0.5% of linearity.

The mirror, in its berylium lightened structure, has been the subject of a numerical analysis of finite elements of vibration methods and the deformations undergone under the influence of the reaction torque of thrusts.

The first vibration mode of the mirror is at 6280 Hz and it appears that in relation to the torque angle characteristics of the thrusts the mirror has no resonance. It simply undergoes deformations at the end of the run which then cancel one another out on the useful part of the scanning.

The maximum values of the deformations at the end of the run can be seen in figure 21, for particular points plotted on a quater mirror (unit : micron).

All the magnetics losses in rotation (hysteresis and eddy current in the thrusts and the pivot) have been calculated and correspond to less than one percent of the maximum rotor kinetic energy.

The compensation of these losses, most of which are reproducible is safeguarded by a torque impulsion that is generated at each cycle by a motor in relation to the gap between the oscillation period and the period of reference.

In this preliminary project, the most serious difficulty is the compensation by the magnetic bearing of the thrusts' instabilities which have been calculated by extrapolating the results of measures taken individually on the test apparatus of figure 16.

Value of axial instability : $K_2 = 1,5 \times 10^6$ N/m

Value of the rotation instability in the mirror : 6.10^4 Nm/Rd

Depending on these two degrees of freedom a great mechanical rigidity must be guaranteed by the stator and the rotor to obtain a good margin of stability for the controls loops of the magnetic bearing.

Evaluations for acceleration , velocity and angular rotation are plotted against the time in figure 22.

CONCLUSION

The main oscillating scanning quality by magnetic thrusts is the reproductibility of the oscillation. Values much lower than 10^{-6} radian can be envisaged. This quality has been confirmed by the preliminary tests carried out.

For the future extrapolations for larger mirrors where higher frequencies are possible.

These perspectives can be taken into account in the drawing up of a new range of futur observation instruments satellite.

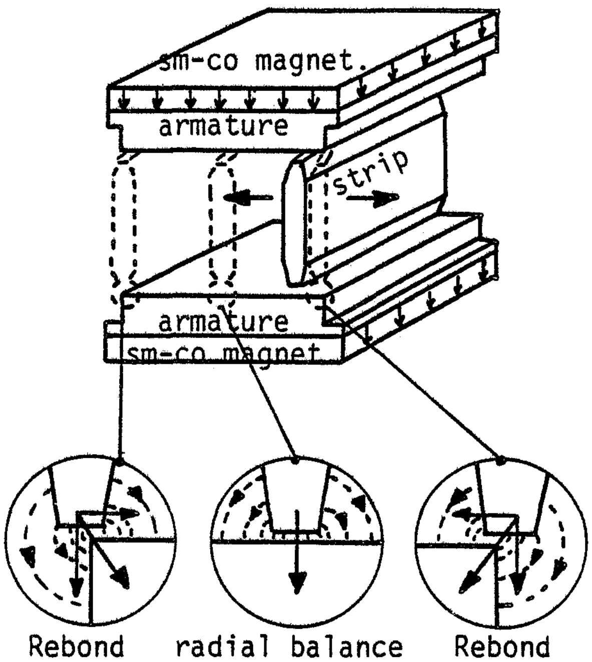

Fig. 1

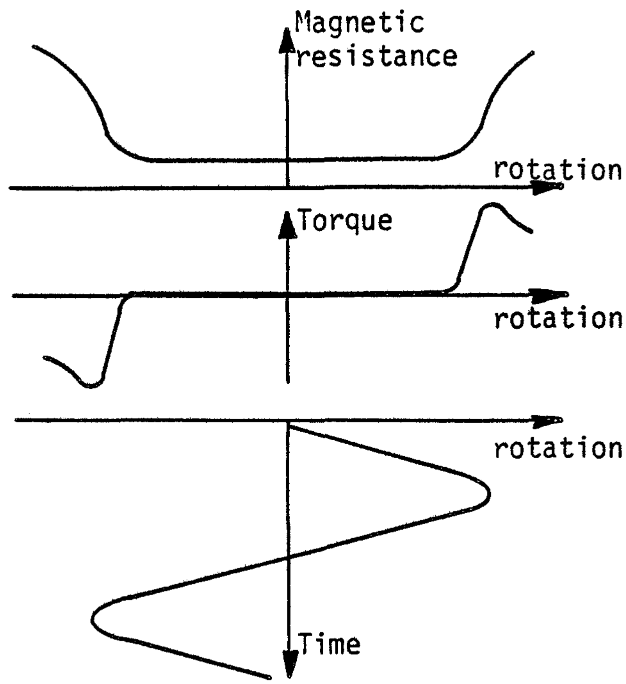

Fig. 2

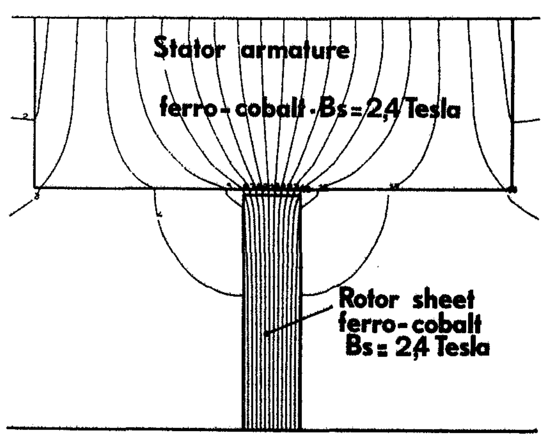

Flux lines distribution

Fig. 3

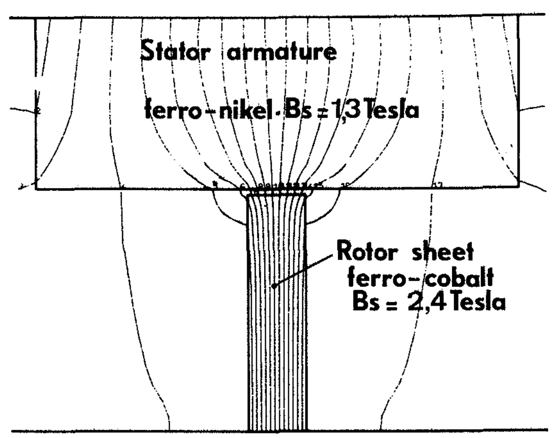

Flux lines distribution

Fig. 4

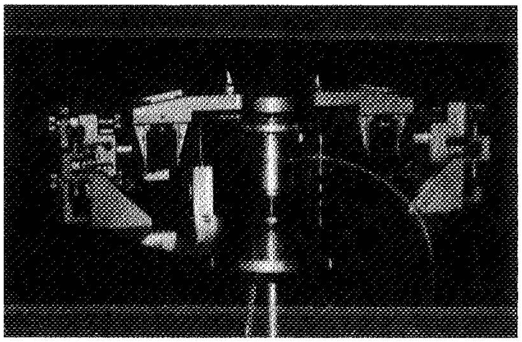

Fig. 5

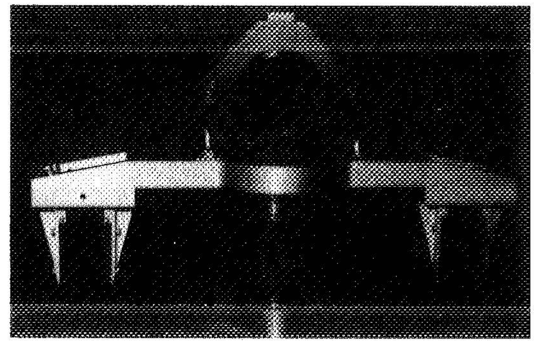

Fig.6

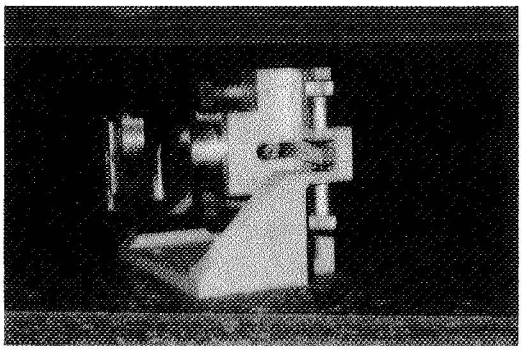

Fig.7

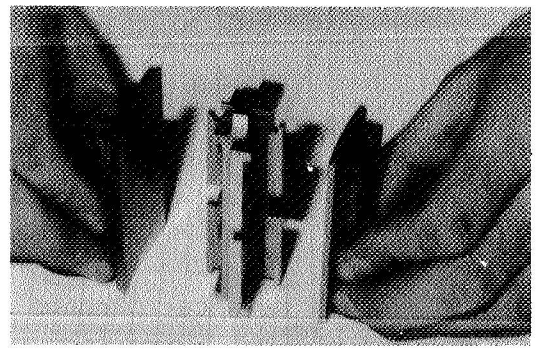

Fig.8

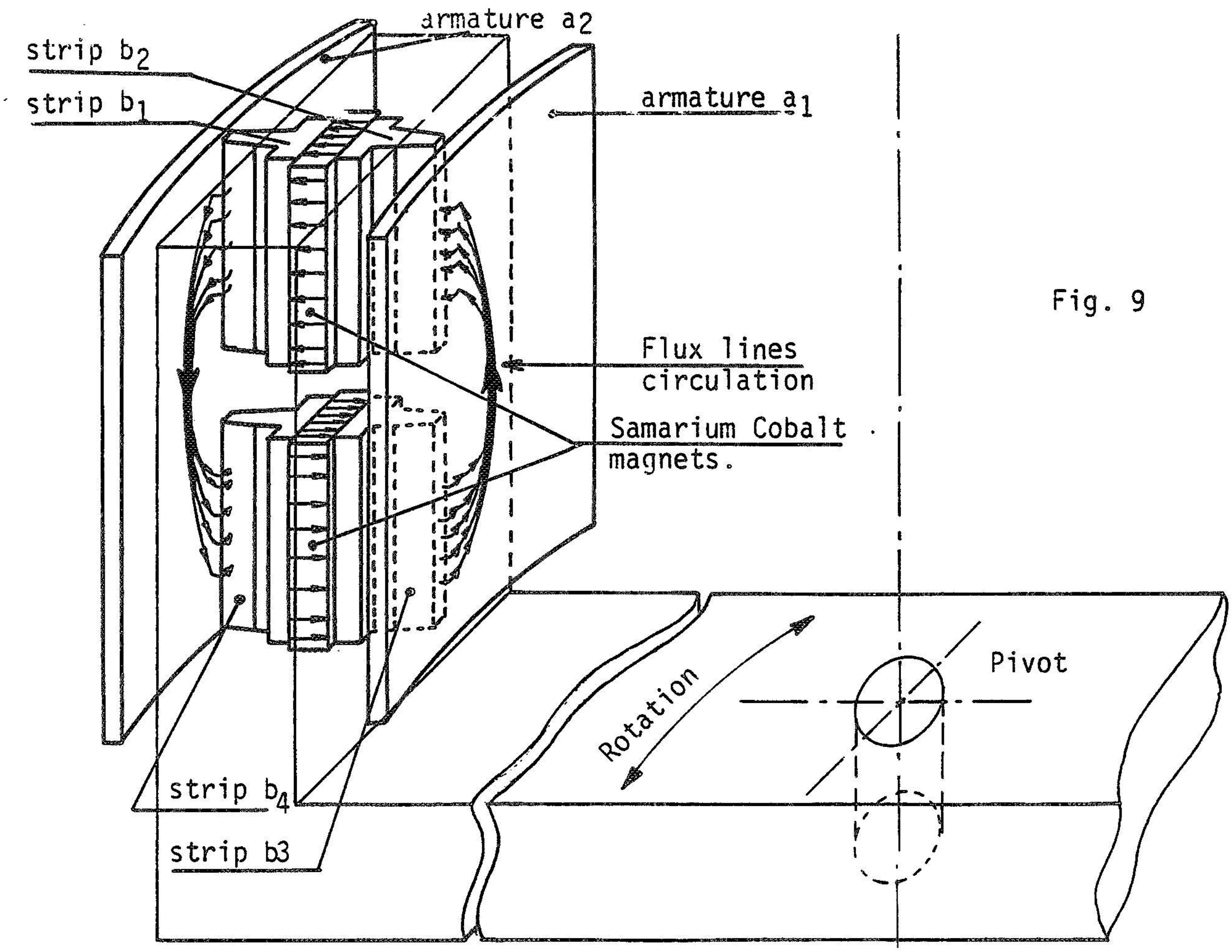

Fig. 9

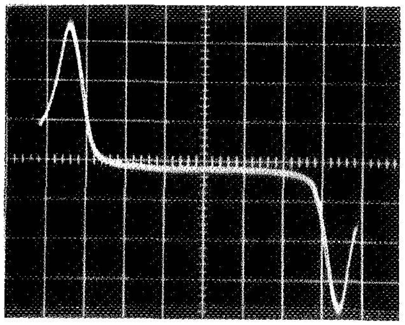

Torque
0,56 Nm/Div

Rotation
1,8 Deg/Div

fig. 10

Rotation
1,8 Deg/Div

Time
50 ms/Div

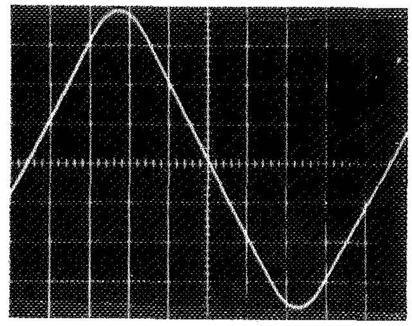

fig. 11

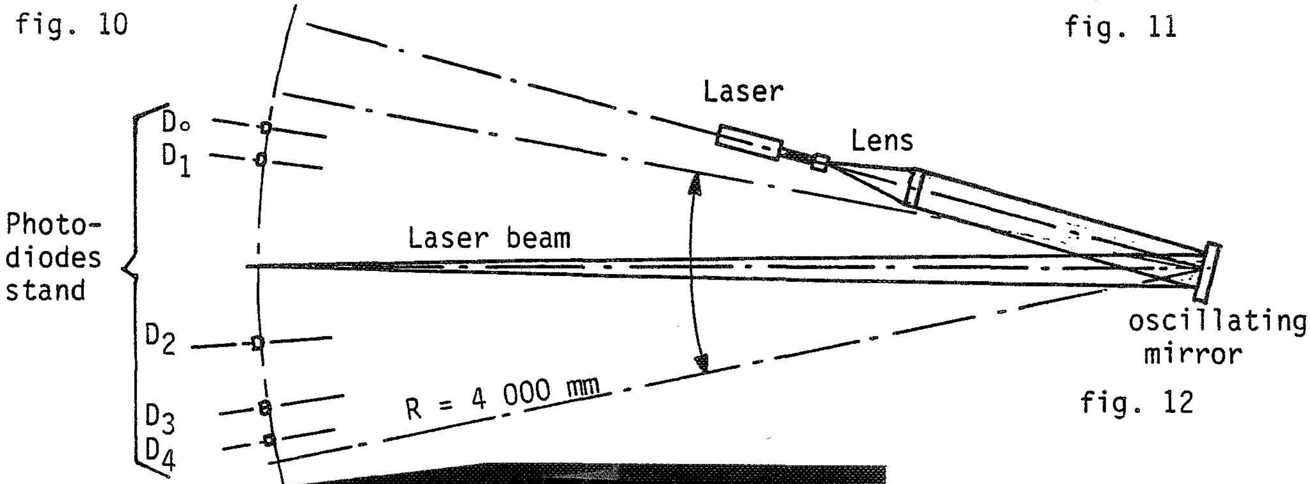

fig. 12

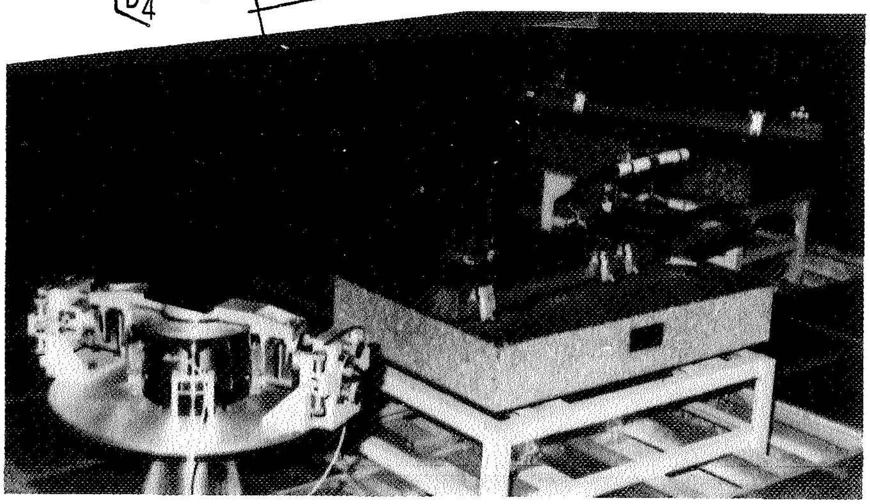

Experimental
laser-control
assembly

fig. 13

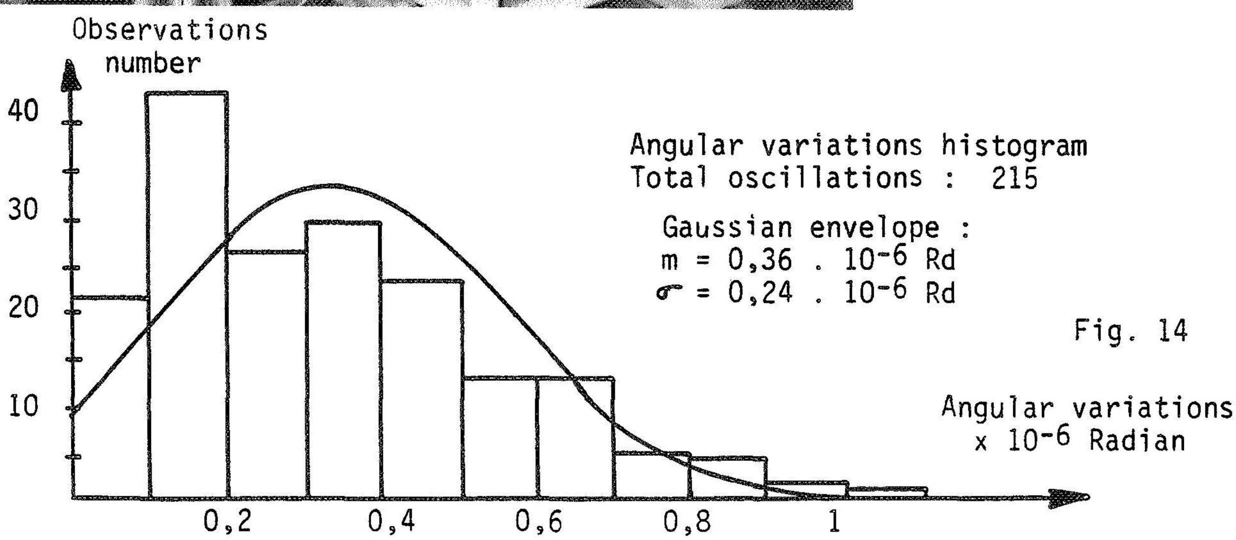

Fig. 14

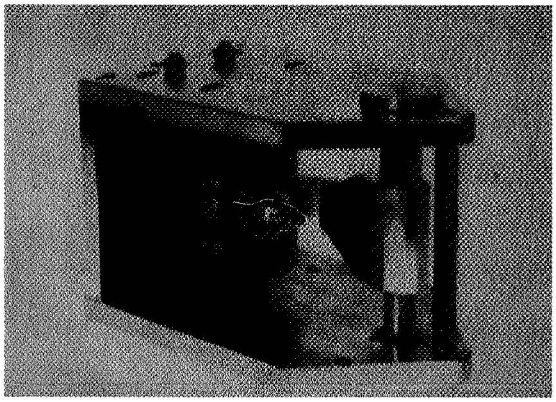

fig:15

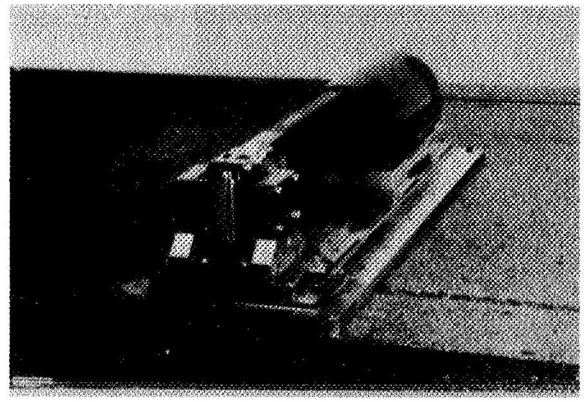

fig:16

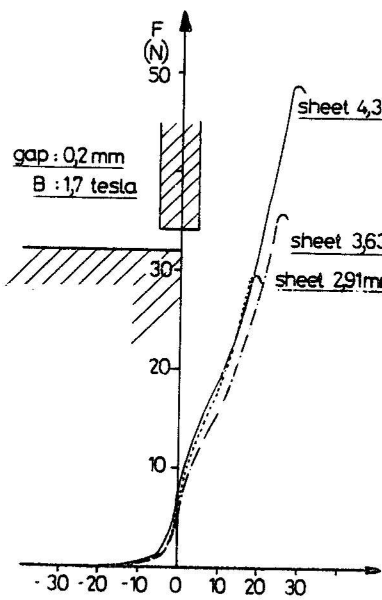

fig:17

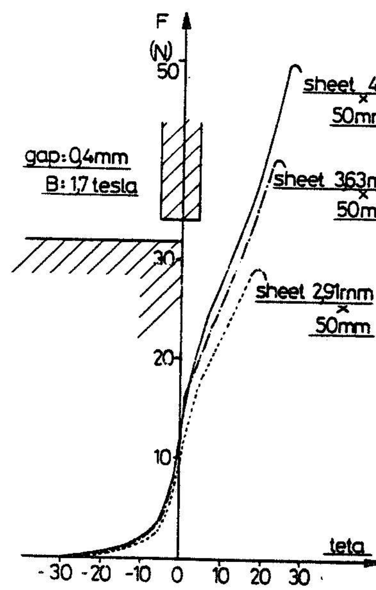

fig:18

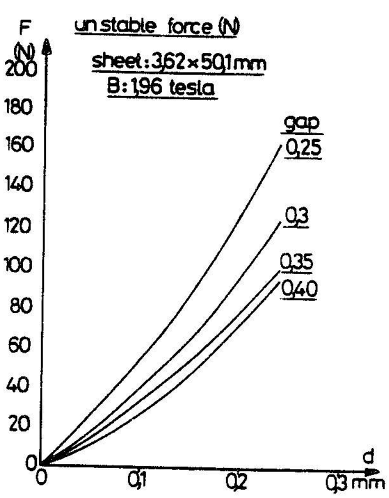

fig:19

fig:20

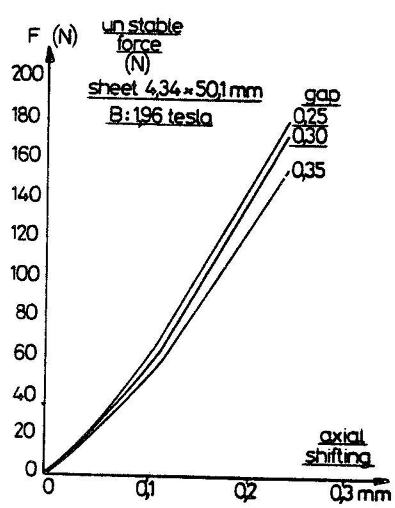

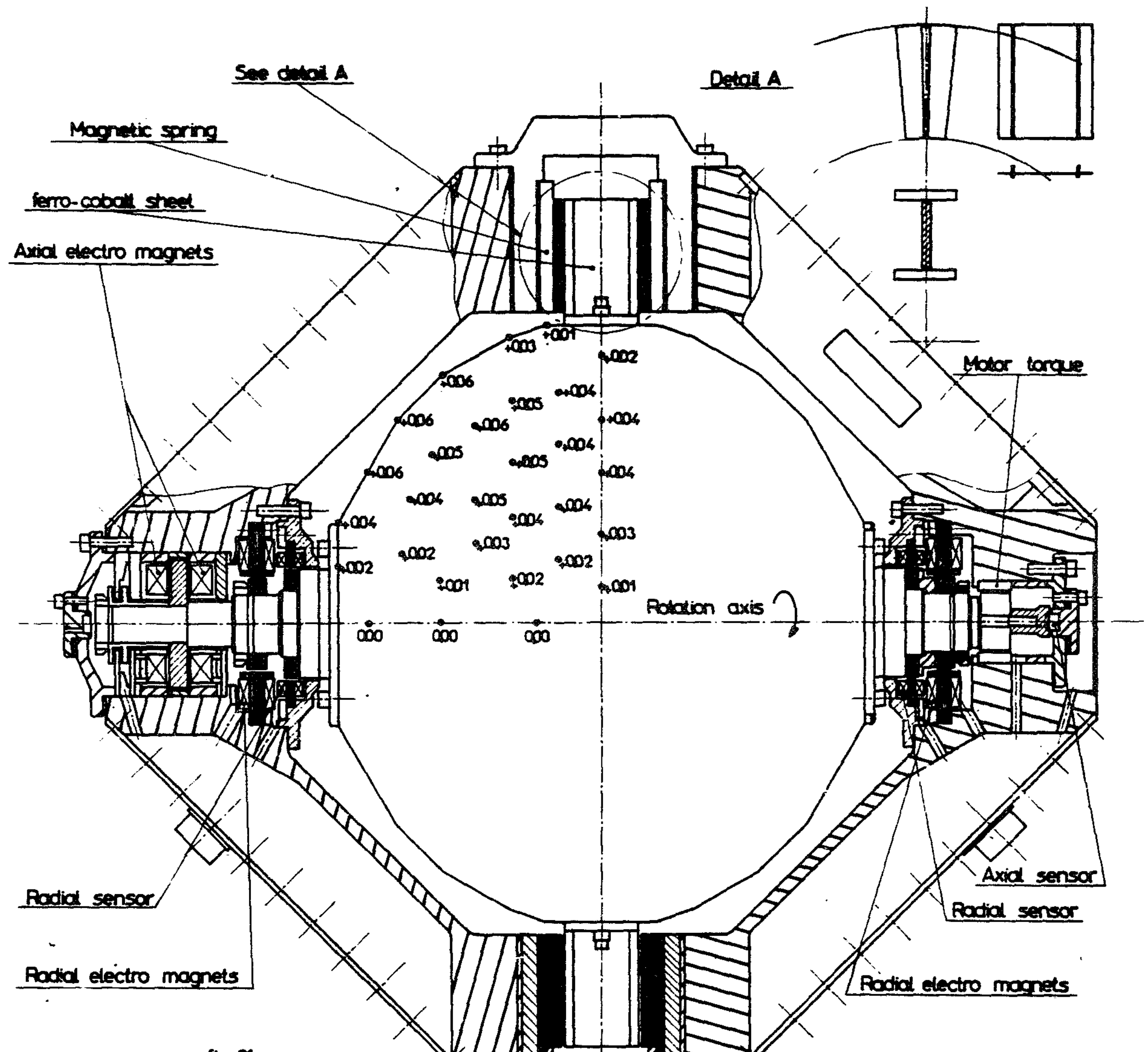
See detail A
Detail A
Magnetic spring
ferro-cobalt sheet
Axial electro magnets
Motor torque
Rotation axis
Radial sensor
Radial electro magnets
Axial sensor
Radial sensor
Radial electro magnets

fig: 21

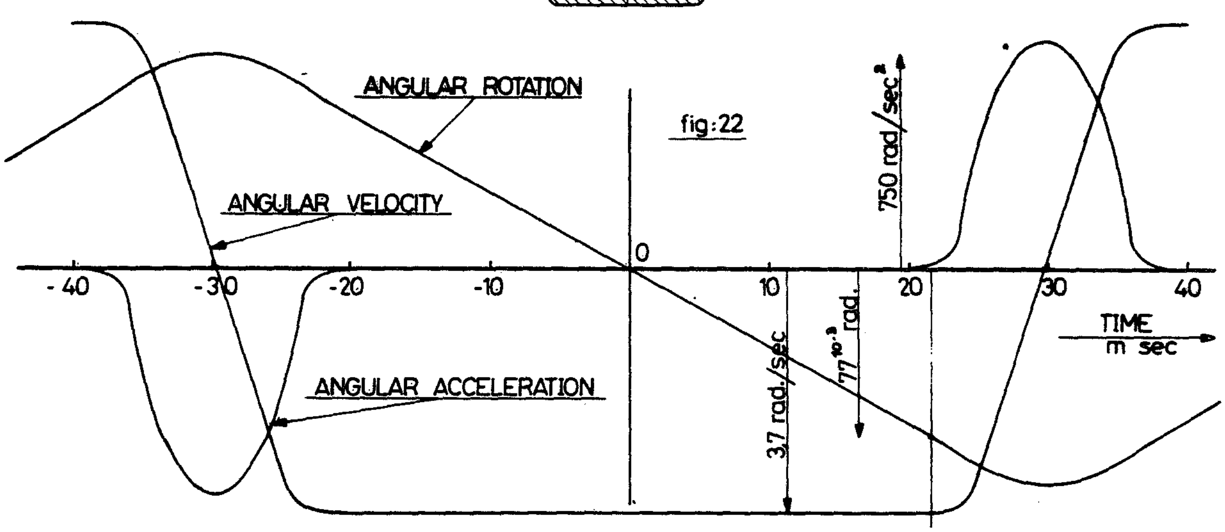
ANGULAR ROTATION
ANGULAR VELOCITY
ANGULAR ACCELERATION
750 rad/sec²
37 rad./sec
77 10⁻³ rad.
TIME
m sec
- 40
- 30
- 20
- 10
0
10
20
30
40

fig: 22